*Tellus* (1986), *38B*, 305–318

# The interaction of mechanically generated turbulence and interfacial films with a liquid phase controlled gas/liquid transport process

By WILLIAM E. ASHER and JAMES F. PANKOW, *Water Research Laboratory, Department of Environmental Science and Engineering, Oregon Graduate Center, 19600 N.W. Von Neumann Drive, Beaverton, OR 97006-1999, USA*

(Manuscript received October 8, 1985; in final form July 8, 1986)

ABSTRACT

The liquid phase rate-controlled transport of $CO_2$ across a gas/liquid interface into water was studied using a non-invasive laser-induced fluorescence (LIF) technique. Turbulence in the liquid layer was generated by a vertically-oscillating grid. The $CO_2$/water interface was cleaned by removal of surface water with additive-free lens paper, or 100% rayon cloth followed by surface vacuuming with a glass Pasteur pipette. The liquid phase mass transfer coefficient $k_L$ was measured under conditions of varying turbulence intensity and scale for each surface cleaning procedure. Transport rates were also measured for an uncleaned surface and in the presence of a deliberately created organic monolayer. All of the results were used to test the surface renewal models of Fortescue and Pearson and Lamont and Scott. A model for wind-dominated gas/liquid transfer developed by Cohen was used to relate the present data to $k_L$ measurements for gas exchange in wind tunnels. This comparison indicates that wind tunnel results may be related to stirred-tank experiments using the turbulent dissipation rate $\varepsilon$, and a surface renewal model.

## 1. Introduction

Gas/liquid transport is an important and complex geophysical process. The aeration of surface waters, the uptake and release of many trace atmospheric gases, and the interaction of increasing levels of atmospheric carbon dioxide with the oceans are all examples of this phenomenon. The rate at which a gaseous species is absorbed by or desorbed from a liquid phase may be controlled in either or both of the 2 phases, and it may show some interfacial or chemical control. When they are rate controlled in one of the two bulk phases and also are free of other effects such as bubbles, gas/liquid exchange processes are mainly dependent on the intensity of the turbulence present in the controlling phase. This makes the understanding of the effect of turbulence on gas/liquid transport of central importance if the detailed modeling of complex natural gas exchange processes is desired.

Since it has been shown that some, if not all, natural water systems have adventitious films at their surfaces (Liss, 1983), the effect of films on gas/liquid transport is also of great importance in the prediction of gas exchange rates. This is the case because surface films will alter the hydrodynamics of the interaction of turbulence eddies with a gas/liquid interface (Davies, 1972).

While the effects of wind will generally dominate natural air/water gas exchange, the process may also be affected by waves, density stratifications, and bubbles. Since the relative importance of these phenomena in their generation of and/or interaction with turbulence is not clearly understood, their consideration in a comprehensive theory of gas/liquid transport has proven to be difficult. This makes the prediction of environmental gas transfer rates from physical data such as wind speed unreliable. It therefore seems fruitful to study a system free from all effects save turbulence and films in the hope of

fully understanding the roles of these two important phenomena in gas/liquid transport. Once this is accomplished, the results could be incorporated into a gas/liquid transfer model for natural bodies of water which takes wind and other such effects into account.

This study provides an examination of the interaction of mechanically-generated liquid phase turbulence of known length and velocity scales with a gas/liquid transport process which is rate controlled in the liquid phase. The effects of various liquid surface cleaning procedures and deliberately formed organic monolayers on the gas exchange process was also studied. A non-invasive laser-induced fluorescence (LIF) technique based on the pH-dependent fluorescence emissions of aqueous fluorescein dyes was used to study the process. This application of LIF to gas transport research allows the exchange process to be sampled with no disruption of the liquid phase turbulence or the gas/liquid interface.

## 2. Theory

### *2.1. Gas exchange overview*

In a gas/liquid exchange process that shows liquid phase control and has both bulk phases well mixed and homogeneous, the flux of the gas across the interface is often given by the empirical equation (Danckwerts, 1970)

$$F = k_L(C_s - C_b), \tag{1}$$

where $F$ (moles cm$^{-2}$ s$^{-1}$) is the flux of gas, $C_s$ (moles cm$^{-3}$) is the liquid phase saturation concentration as determined by Henry's Law, $C_b$ (moles cm$^{-3}$) is the concentration in the bulk phase of the liquid and $k_L$ (cm s$^{-1}$) is the liquid phase mass transfer coefficient. $C_s$ depends upon the identity and the partial pressure of the gas involved, and also upon the temperature. $C_b$ is a function of time inasmuch as it is a measure of how far the bulk system is from equilibrium. The hydrodynamical dependence of the process resides in $k_L$. Therefore it is $k_L$ which is of primary importance in this study.

The explicit hydrodynamical dependence of $k_L$ depends on the cleanliness of the gas/liquid interface. Turbulent eddies near a film-covered gas/liquid interface are damped differently than eddies close to a film-free surface (Davies, 1972). Since it is the eddies which come closest to the interface which have the greatest influence on gas exchange, this change in damping may have a profound effect on gas/liquid transport. Also, certain kinds of films have been shown to create a chemical barrier to transport (Springer and Pigford, 1972). Each of these properties of surface films may affect the transport process. Therefore, the film-free and film-covered interfaces must be treated separately since they are hydrodynamically different and may be chemically distinct as well.

### *2.2. Film-free gas/liquid interfaces*

Liquid-phase turbulence velocity fluctuations parallel to the interfacial plane do not create large shear stresses at a film-free gas/liquid interface. The mobility of the liquid at the interface permits these fluctuations to persist up to the actual liquid surface. However, in the direction normal to the interface the liquid damps velocity fluctuations through surface tension and gravity. Therefore, the vertical velocity component at the interface must go to zero provided that the turbulence eddies do not penetrate the interfacial plane. Visualization of turbulence at an air/water interface has shown that this is an accurate description of eddy motion at a clean surface (Davies, 1972). Therefore, models which describe gas/liquid transport at a clean interface should take this behavior into account.

Surface renewal models of gas/liquid transport describe the process in a manner that is phenomenologically consistent with the observed behavior of the turbulence. As proposed by Higbie (1935) and extended by Danckwerts (1970), surface renewal theory models the transfer process by assuming that patches of the surface are periodically replaced by fluid elements from the well-mixed bulk phase below. Gas is transferred to or from these elements by molecular diffusion while they are at the interface. Higbie's original theory makes the assumption that all fluid elements have equal residence time at the interface. If this residence time is $\tau$ ($s$), then $k_L$ may be written as (Higbie, 1935)

$$k_L = 2(D/\pi\tau)^{1/2}, \tag{2}$$

where $D$ (cm$^2$ s$^{-1}$) is the diffusion coefficient of the gas in the liquid. Danckwerts (1970) assumed that there was a stationary distribution of surface

element lifetimes. The fraction $s$ ($s^{-1}$) of surface area replaced in unit time or surface renewal rate is computed from this distribution. Then,

$$k_L = (Ds)^{1/2}. \tag{3}$$

In (2) and (3), the dependence of $k_L$ on the turbulence is present implicitly in $\tau$ and $s$ respectively. Models based on surface renewal theory which deal with the explicit character of this dependence have been developed by Fortescue and Pearson (1967) and Lamont and Scott (1970).

Fortescue and Pearson (1967) argued that for a system of regular large eddies,

$$k_L = 1.46(DQ/L)^{1/2} \tag{4}$$

where $L$ (cm) is the integral turbulent length scale (Tennekes and Lumley, 1972) and $Q$ (cm $s^{-1}$) is defined as the square root of twice the average turbulent kinetic energy, i.e.,

$$Q = (u'^2 + v'^2 + w'^2)^{1/2}, \tag{5}$$

where $u'$, $v'$, and $w'$ (cm $s^{-1}$) are the mean turbulent velocity fluctuations in the x, y, and z directions, respectively.

Lamont and Scott (1970) used a model based on the small scale motions present in an eddy cell to predict $s$. With this model and the Kovasznay turbulent energy spectrum (Hinze, 1975), they arrived at the following expression for $k_L$

$$k_L = 0.4(\varepsilon\nu)^{1/4}\mathrm{Sc}^{-1/2} \tag{6}$$

where $\nu$ ($cm^2$ $s^{-1}$) is the kinematic viscosity, Sc is the dimensionless Schmidt number of the fluid defined by

$$\mathrm{Sc} = \nu/D \tag{7}$$

and $\varepsilon$ is the turbulent energy dissipation rate which is defined as power per unit mass of fluid ($cm^2$ $s^{-3}$). $\varepsilon$ may be estimated in terms of $Q$ and $L$ as (Tennekes and Lumley, 1972)

$$\varepsilon = AQ^3/L \tag{8}$$

where $A$ is a constant which Mellor (1973) found to be equal to 1/15.5.

Both the Fortescue and Pearson (1967) model and the Lamont and Scott (1970) model provide a method of relating gas transport coefficients to turbulence parameters which may be measured in the laboratory. They provide a means to test surface renewal gas/liquid transport models. However, surface renewal models are not necessarily valid for film-covered gas/liquid interfaces.

### *2.3. Film-covered gas/liquid interfaces*

Organic films on gas/liquid interfaces resist deformation and spreading. Therefore, their presence causes greater tangential stresses than found at a clean interface. This increase in stress leads to an increase in the damping of the turbulence motions at the surface. In fact, a severely contaminated interface will not allow velocity fluctuations in the interfacial plane. Since this is hydrodynamically analogous to a solid/liquid interface, transport at a film covered gas/liquid interface is described in this limiting case by hydrodynamical relations similar to those for solid/liquid interfacial transport (Davies, 1972).

Solid/liquid transport is postulated to be controlled by a diffusive sublayer in the laminar layer of the solid/liquid boundary. Solid/liquid transport models define $k_L$ in terms of $D$ and this diffusive sublayer depth. Relations of this type have been derived by Whitman (1923) and Levich (1962). Empirical correlations based on these results have shown that (Davies, 1972)

$$k_L = 0.13(\varepsilon\nu)^{1/4}\mathrm{Sc}^{-2/3}. \tag{9}$$

While comparison of (6) to (9) would appear to show that the clean and film-covered interface transport regimes are hydrodynamically equivalent (i.e., same functional dependence on $\varepsilon$), this is not the case. The difference in proportionality constants and dependence on Sc in (6) and (9) leads to a fundamentally different fluid mechanical interpretation of each.

If the surface is partially contaminated or the organic material is weakly surface active, it is expected that the hydrodynamical dependence will fall somewhere between the clean gas/liquid and solid/liquid cases (Davies, 1972). Therefore, it is not expected that the clean surface models embodied by (4) and (6) or the film-covered model realized in (9) will fully describe the transport process for an interface with a partial or weak surface film. These models provide the limiting behavior of a gas/liquid transport system.

## 3. Available experimental techniques

Most laboratory work in this area has been carried out using wind tunnels, stirred cells,

and/or moving bands or films. The majority of the recent work has been performed with wind tunnels and stirred cells. In wind tunnel studies, gas is blown over a layer of liquid. Both linear and circular wind tunnels have been used. The measured value of $k_L$ is then related to such parameters as the friction velocity or wind speed. While fairly common, such studies are often complicated by the presence of waves and bubbles. In circular wind tunnels, there are also complicating effects due to the circular motion of the air and water. This motion with its accompanying constant centripetal acceleration creates cyclical roll cells across the liquid layer which may enhance the transfer rate (Jähne et al., 1979). The cells also cause problems in turbulence measurement and characterization.

A stirred cell apparatus consists of a tank of water with a headspace in which the transferring gas(es) is (are) introduced. Either invasion or evasion may be studied. The mixing in the liquid phase is generally varied to produce changes in $k_L$. This stirring is usually intense enough to ensure that the bulk fluid is well mixed. Commonly used stirrers are rotating impellers (Davies and Lozano, 1979), recirculation pumps (Balls and Liss, 1983) and vertically-oscillating grids (Dickey et al., 1984). The main drawback to rotary-stirred and pump-mixed experiments is that the turbulence generated is non-homogeneous. This means that the turbulent length and velocity scales present at the fluid interface are not spatially uniform. This is a serious deficiency if surface renewal models are to be tested. It is also difficult to relate different experiments to each other since the turbulence generated by rotating stirrers and jets is highly dependent on the tank geometry, stirrer dimension, jet orifice size, and jet or stirrer velocity.

In contrast, a vertically-oscillating grid may be used to produce turbulence at a gas/liquid interface. Experimental evidence exists to show that the turbulence so generated is isotropic in the interfacial plane and may be related between different experiments and laboratories (Thompson and Turner, 1975; Hopfinger and Toly, 1976; Brumley, 1984; Dickey et al., 1984). Grids also have been shown to generate turbulence whose length and velocity scales may be related to easily measured parameters such as oscillation frequency $\omega$ (Hz), stroke length $s'$ (cm), and depth (Thompson and Turner, 1975; Hopfinger and Toly, 1976; Brumley, 1984; Dickey et al., 1984).

Hopfinger and Toly (1976) studied the turbulence generated by a grid of bars with square cross section. They found that for a flat grid of square bars with a ratio of bar cross section $d$ (cm) to grid mesh spacing $M$ (cm) of 1 to 5, $u'$, $v'$, $w'$, and $L$ could be related to $\omega$, $s'$, $M$, and the distance from the virtual origin $Z$ by

$$u' = v' = CM^{1/2}s'^{3/2}\omega Z^{-1}, \tag{10}$$

$$w' = 1.25u', \tag{11}$$

$$L = \beta Z, \tag{12}$$

where $C$ and $\beta$ are known dimensionless functions of $M$ and $s'$ and $Z$ lies 0.5 cm below the mid-stroke grid position for a grid with $M = 5$ cm and $d = 1$ cm. This type of grid seems well suited to gas transfer research since it allows the generation of turbulence with known, reproducible scales.

Unfortunately, the water surface in a grid-stirred tank is prone to form adventitious surface films. These films are composed of organic matter which was (1) originally dissolved in the bulk liquid phase and/or (2) deposited from the gas phase. Therefore, extreme care must be taken in the preparation of the tank water so that these effects will be minimized. Precautions may include purification of the bulk aqueous phase and cleaning of the water surface prior to an experiment.

Scott (1975) suggests that surface active contaminants may be removed from aqueous solutions by purging with He bubbles. The He bubbles will concentrate these compouds at the interface. The interface must then be cleaned by removal of the surface water. This technique, along with scrupulous cleaning of the actual grid and tank should allow the effects of surface films to be minimized. The measurement of gas transfer rates after the deliberate creation of a controlled monolayer on the interface can provide a reference for determining when adventitious films are present.

Sampling should be done in a manner which does not generate or disrupt turbulence in the liquid, or disturb the gas/liquid interface. The development of a non-invasive method for studying the gas/liquid transport process requires that

the system react to produce an easily-measured product. Such a system is provided by carbon dioxide and water. The hydration of $CO_2$ to the weak acid $H_2CO_3$ allows pH to be used as a mass transfer indicator. It has simple aqueous phase rate control for pH < 5 (above pH = 5 the transport of bicarbonate ($HCO_3^-$) and carbonate ($CO_3^{2-}$) ions become increasingly important). The only limitation is that the hydration rate is relatively slow (rate constant = $3.8 \times 10^{-2}$ $s^{-1}$, Gibbons and Edsall, 1963). Since the attainment of the equilibrium pH requires the presence of hydration equilibrium, care must be taken so that the formation of $H_2CO_3$ is not rate limiting.

The total concentration of $CO_2$ species $C_b$ (moles $cm^{-3}$) is determined from the pH by

$$C_b = \{(C_B - C_A + [H^+] - [OH^-])/(a_1 + 2a_2)\}, \quad (13)$$

where $C_B$ (moles $cm^{-3}$) is the amount of mineral base present, $C_A$ (moles $cm^{-3}$) is the amount of mineral acid present, and $a_1$ and $a_2$ are known, dimensionless functions of the pH, temperature $T$ (°C), acidity constants, and ionic strength $I$ (moles $cm^{-3}$) (Stumm and Morgan, 1982).

Use of (1) and making the assumption that the bulk aqueous phase is homogeneous allows the concentration change with time to be written as

$$dC_b/dt = \{k_L/h\}(C_s - C_b), \quad (14)$$

where $h$ (cm) is the height of the water column. Integration of (14) yields

$$\{k_L/h\}t = -\ln\{(C_s - C_b)/C_s\} \quad (15)$$

where it has been assumed that $C_b = 0$ at $t = 0$. Therefore, when (1) describes the mass transport process, linear regression of $-\ln\{(C_s - C_b)/C_s\}$ versus $t$ will give a straight line with a slope of $k_L/h$.

The non-invasive pH measurement technique developed by Pankow et al. (1984) to avoid the problems associated with pH electrode use relies on the pH-dependent fluorescence emissions of fluorescein dyes. This approach was first used by Ohkuma and Poole (1978) to study the pH of living cells. It utilizes the acid-base chemistry of the fluorescein structure in aqueous solution. Fluorescein may exist predominately as a cation, a neutral quinoid, a mono-anion, or a dianion, depending on the solution pH (Lindqvist, 1960). Since the mono-anion and dianion exhibit the most intense fluorescence and predominate at higher pH values, increasing the pH permits increasing fluorescence emissions. The pH range where the maximum fluorescence intensity change occurs can be controlled somewhat by the substitution of chlorines for hydrogens on fluorescein's aromatic rings. Due to the electrophilic character of chlorine, this tends to lower the pH transition range. Since the pH must be kept relatively low to keep $CO_2$ mass transfer simple, the compound chosen for this particular study was 2′,7′-dichlorofluorescein (DCFS). Its maximum change in fluorescence occurs in the pH range 3.5 to 6.0.

The preferred light source for fluorescence excitation is the laser. It provides intense, monochromatic light and its coherent beam gives excellent spatial resolution. These features allow the fluorescence measurements to be made by simple optical filtering procedures. An additional advantage is that the detection limits for fluorescein and its derivatives by LIF are extremely low. Lytle (1982) reported a minimum detection limit of $10^{-13}$ moles $cm^{-3}$ for fluorescein in basic aqueous solution. This is important for this application since the concentration of the DCFS must be low enough that $CO_2$ species dominate the acid/base chemistry.

## 4. Experimental

The apparatus used is shown schematically in Fig. 1. It consisted of a square horizontal cross-section tank of water with a headspace for the transporting gas, a rack made from 0.3 cm thick, 2.5 cm square steel tubing, and a vertically-oscillating grid. The dimensions of the tank and grid, as well as the construction materials were the same as those used by Thompson and Turner (1975). To minimize mechanically-generated ripples on the $CO_2$/water interface, the rack was constructed so that the tank lid, grid and grid drive train did not touch the walls of the tank. The grid support shafts were isolated from the gas/water interface by stainless steel sleeves. Careful construction and alignment of the system prevented lateral movement and twisting of the grid during operation.

The range for $\omega$ was 2 to 6 Hz, and the range for $Z$ was 7.5 to 18 cm. The value of $s'$ was either 1.5 or 2.5 cm. The grid had the same $d$ and $M$ as

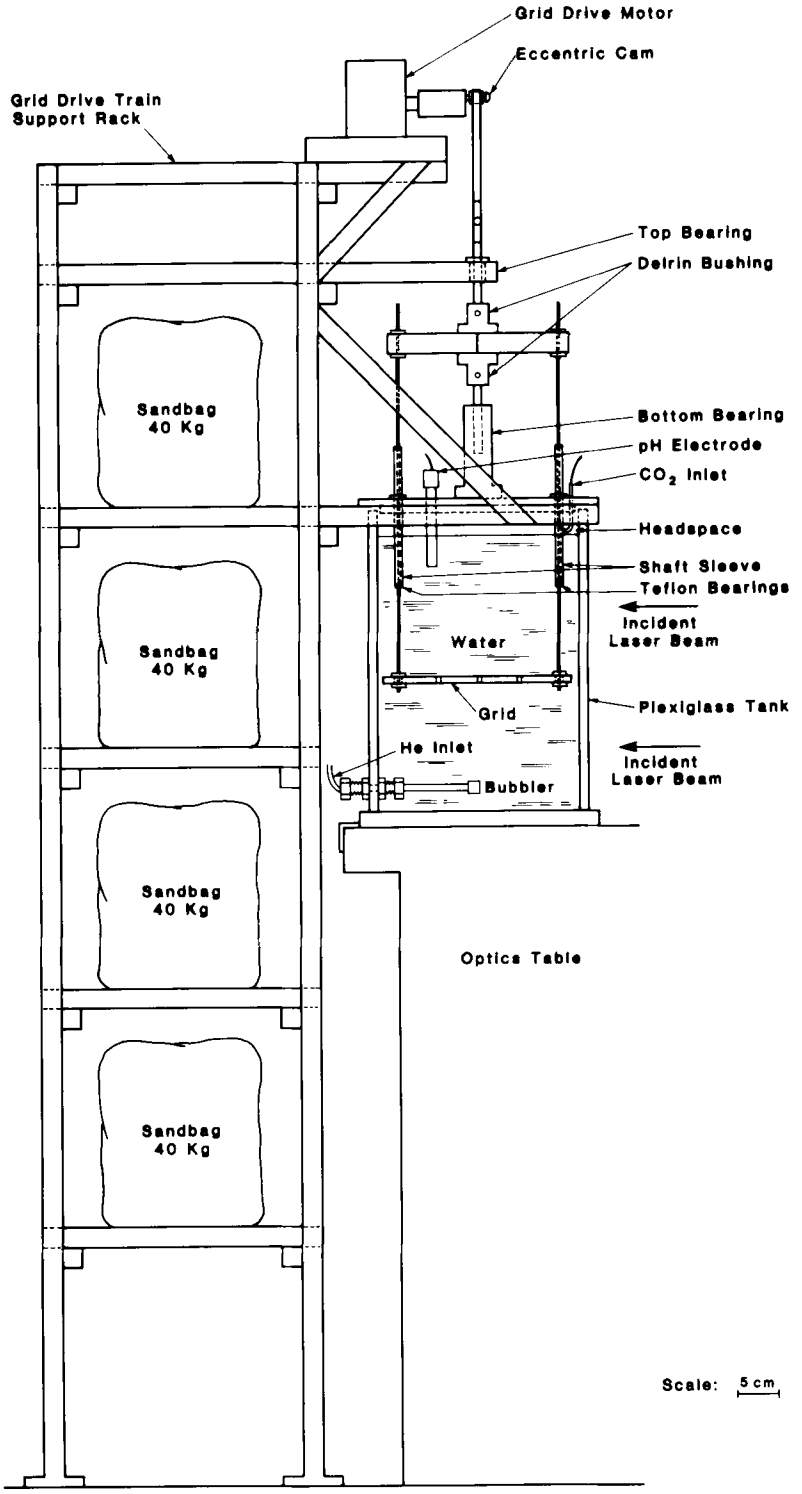


*Fig. 1.* Diagram of the experimental apparatus showing tank, grid and grid drive train. LIF optics not shown.

that used by Hopfinger and Toly (1976) who found that $C = 0.2$ and that $\beta$ varied from 0.13 to 0.18 for $s'$ varying from 1.5 cm to 2.5 cm. By applying (10), (11) and (12) it was found that these conditions gave calculated turbulent Reynolds numbers ($Re_t$) from 40 to 400.

The excitation light was provided by the 488 nm line of a Coherent Radiation Laboratory (Palo Alto, CA) CR-3 argon ion laser. Prior to entering the tank, the incoming laser beam was split into two beams using a plate beamsplitter. The positions of the two beams were adjusted using mirrors so that they entered the tank perpendicularly to the incident face, and propagated through the tank at horizontal depths of 5 and 25 cm. The two beams were sampled concurrently at their mid-tank positions. Dual sampling was carried out to monitor the bulk liquid homogeneity. Each beam's fluorescence emission was monitored perpendicularly to the incident laser light to minimize noise from scattered laser radiation. A bandpass optical filter with a half-bandwidth of 8 nm centered on the fluorescence maximum at 525 nm was used to separate fluorescence radiation from scattered 488 nm laser light. The fluorescence emissions were measured using a Hammamatsu (San Jose, CA) S1223-BR photodiode and a Burr-Brown (Tucson, AZ) OP121A operational amplifier. The response time of the photodiode-amplifier combination was approximately 0.01 s.

Deionized water, which had its pH set at 5.0 by addition of small amounts of dilute HCl or $CO_2$-free NaOH, was first added to the dissolution cell. The value of $I$ was adjusted to $1 \times 10^{-5}$ moles cm$^{-3}$ using reagent grade NaCl which had been heated to 500°C to remove adsorbed organic material. This provided a constant $I$ during the course of an experiment. The DCFS concentration in all runs was $6 \times 10^{-10}$ moles cm$^{-3}$. Experiments and calculations have shown this concentration to be a good balance between signal detection and chemical interference. The temperature of the water was allowed to equilibrate with the room temperature which was between 20 and 23°C. (Once stabilized, it remained constant during the course of an experiment.) The bulk liquid and headspace were then purged of $O_2$ and $CO_2$ by bubbling filtered He (0.4 $\mu$m HEPA, Gelman Sciences, Ann Arbor, MI) through the water column. This procedure also removed surface active contaminants from the aqueous phase.

Prior to the start of an experiment, the water surface was cleaned by removal of surface water with one of two procedures. The first employed sheets of additive-free lens paper (Fisher Scientific, Springfield, NJ) and the second used 100% rayon cloth (Fisher Scientific, Springfield, NJ) followed by surface "vacuuming" with a glass Pasteur pipette connected to a peristaltic pump. After cleaning, the water was tested for surface active compounds by use of the Crits ring test (Crits, 1961). In no case did this test show significant levels of such materials.

As a further check on surface contamination several experiments were performed with either no cleaning, or with a 1-octadecanol (1-OD, 95% grade, Aldrich Chemical Co., Milwaukee, WI) monolayer on the water surface. The monolayer was formed by pipetting 0.07 cm$^3$ of an $8 \times 10^{-6}$ moles cm$^{-3}$ solution of 1-OD in n-pentane onto the water surface and evaporating the pentane using dry $N_2$ gas. After these experiments were completed, the tank, grid and grid drive train were thoroughly washed to prevent 1-OD from being present during subsequent experiments.

During calibration only, a pH electrode was inserted into the tank via a port in the cover. pH was measured with an Orion Research (Cambridge, MA) 701A Digital Ionalyzer calibrated with NBS buffers at pH 4, 5, and 6. The fluorescence emissions were calibrated as a function of pH and incident laser power. The incident power calibration allowed fluorescence measurements made at different incident laser intensities to be related to each other. In particular, since the incident power versus fluorescence calibration was shown to be linear, all power corrections were done by ratio to a reference power level. Each pH versus fluorescence calibration curve was fit to a third order polynomial of the form

$$\mathrm{pH} = A_0 + A_1 S + A_2 S^2 + A_3 S^3, \tag{16}$$

where $S$ represents the fluorescence signal value in arbitrary units. This was done using a least squares regression. A correlation coefficient of 0.9995 for the power-corrected fluorescence intensities was typically obtained. The standard error of the fit was typically 0.01 pH units. A typical pH versus fluorescence calibration is

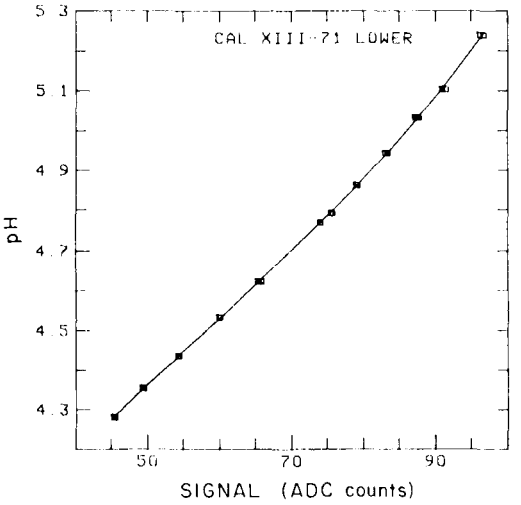


*Fig. 2.* Plot of typical pH versus fluorescence calibration where fluorescence intensity was measured in analog/digital converter (ADC) counts. □, calibration data points, solid line, 3rd order linear regression of data. From (16) in text, $pH = 3.076 + 0.03964S - (3.860 \times 10^{-4})S^2 + (2.152 \times 10^{-6})S^3$. The correlation coefficient ($r$) was 0.9999 and the standard error of the fit was ±0.005 pH units. Experimental code XIII-71.

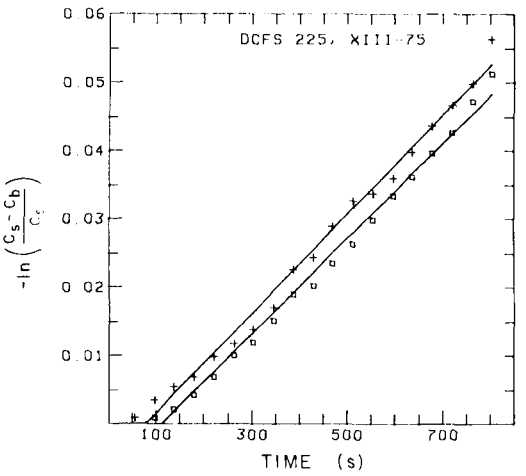


*Fig. 3.* Typical plot of $-\ln\{(C_s - C_b)/C_s\}$ versus $t$ for $CO_2$ invasion experiment with dual sampling at depths of 5 and 25 cm. +, upper beam data, solid line is linear regression with slope ($m$) = $7.3 \times 10^{-5}$ s$^{-1}$, $r = 0.997$. □, lower beam data, solid line is linear regression with $m = 7.0 \times 10^{-5}$ s$^{-1}$, $r = 0.996$. Experimental code XIII-75, DCFS #225.

presented in Fig. 2. pH was predicted from fluorescence measurements with a precision of ±0.02 pH units (±1$s$) determined by a linear regression of predicted versus electrode measured pH values.

During an experiment, dry filtered (0.4 μm HEPA) $CO_2$ gas (Airco, Vancouver, WA, 2.8 grade) was admitted into the tank headspace and the resulting fluorescence changes were recorded by a computer data acquisition system. The bulk fluid pH was measured immediately before and after each experiment. This allowed corrections to be made for DCFS photodecomposition.

For each experiment, the raw fluorescence data was first power-ratioed to correct for laser power drift. The pH was then calculated using (16). Since $C_A$ was known from the starting pH and $C_B$ was 0, $C_b$ was calculated from (13). Application of (15) required that $C_s$ be calculated based on Henry's law and a measurement of the atmospheric pressure. The data was then plotted as discussed for (15), and a linear regression performed. Calculation of $k_L$ was then trivial as $h$ was easily measured and the slope was known from the linear regression. A typical plot of this type is shown in Fig. 3. The upper and lower beam data indicated that the tank was homogeneous to within experimental error.

Literature values of $D$ for $CO_2$ in pure $H_2O$ were used. In the temperature range of these experiments the value for $D$ was $1.76 \times 10^{-5}$ cm$^2$ s$^{-1}$ (Ackgerman and Gainer, 1972).

## 5. Results and discussion

The precision of $k_L$ was found by using standard propagation of errors starting from a relative uncertainty in $[H^+]$ of ±4% (±1$s$) and assuming that all other uncertainties were negligible. The standard formulas for the uncertainties in linear regression coefficients were used (Bevington, 1969). The values for $k_L$ and their calculated uncertainties for the data shown in Fig. 3 were $2.6 \times 10^{-3} \pm 0.4 \times 10^{-3}$ and $2.5 \times 10^{-3} \pm 0.4 \times 10^{-3}$ cm s$^{-1}$ for the upper and lower beams, respectively.

Since the turbulence scales in the tank and at the $CO_2$/water interface were not measured directly, it was assumed that they could be estimated by (10), (11) and (12). However, the experiments of Brumley (1984) and Dickey et al. (1984) have shown that these equations do not fully describe the behavior of the turbulence scales close to a gas/liquid interface. Therefore, they were modified in the following manner

for the interfacial region. Brumley's (1984) data showed that $w'$ goes to zero at the interface while $u'$ is reasonably estimated by (10). This result was to be expected if there was no surface distortion caused by the turbulence (Hunt and Graham, 1978). Since minimal distortion was observed in the present experiments, $Q$ was calculated at the surface by assuming $w' = 0$ and $u' = v'$ where $u'$ was given by (10). Dickey et al. (1984) showed that although the presence of a gas/liquid boundary affects the linear relation of $Z$ with $L$, the deviation from linearity at the interface is approximately 10%. This error was felt to be acceptable and (12) was used to calculate $L$ using the constants of Hopfinger and Toly (1975).

The experimentally determined $k_L$ values were grouped by similar turbulence parameters and aqueous surface preparation technique (i.e., no cleaning, lens paper-cleaned, rayon- and vacuum-cleaned, and 1-OD monolayer-covered). The $k_L$ values from experiments with similar conditions were then averaged. These average $k_L$ values were then plotted against $(DQ/L)^{1/2}$ and $(\varepsilon\nu)^{1/4}Sc^{-1/2}$. This tested the validity of the two clean-interface surface renewal models represented by (4) and (6). These plots are shown in Figs. 4 and 5. In both figures $Q$, $L$ and $\varepsilon$ were computed at the interface from (8), (10) and (12).

The experiments where the water surface was cleaned show no significant increase of $k_L$ with increasing turbulence intensity until a critical value of $(DQ/L)^{1/2}$ or $(\varepsilon\nu)^{1/4}Sc^{-1/2}$ is reached. At higher turbulence intensities, the correlation is linear as predicted by (4) and (6). In the rayon/vacuum cleaned data set this transition occurs where $(DQ/L)^{1/2} \simeq 1.9 \times 10^{-3}$ cm s$^{-1}$ and $(\varepsilon\nu)^{1/4}Sc^{-1/2} \simeq 3.0 \times 10^{-3}$ cm s$^{-1}$. The transition in the lens paper-cleaned results occurred where $(DQ/L)^{1/2} \simeq 2.5 \times 10^{-3}$ cm s$^{-1}$ and $(\varepsilon\nu)^{1/4}Sc^{-1/2} \simeq 4.5 \times 10^{-3}$ cm s$^{-1}$.

This transition may be explained if the scale relations given by (10), (11) and (12) become non-applicable for low turbulence intensities. If the calculated turbulence scales are accurate however, this transition may imply that for weak turbulence the models represented by (4) and (6) do not adequately describe the transport process. This may be due to eddies at the lower turbulence levels not having the dynamic thrust necessary to renew the gas/liquid interface. If this interpretation is correct it implies that both the lens paper- and rayon/vacuum-cleaned surfaces behaved like film-covered interfaces at low turbulence intensities. This behavior might have been caused by the presence of weak surface films. At higher levels of turbulence, the eddies were energetic enough to penetrate the film and cause renewal of the interface.

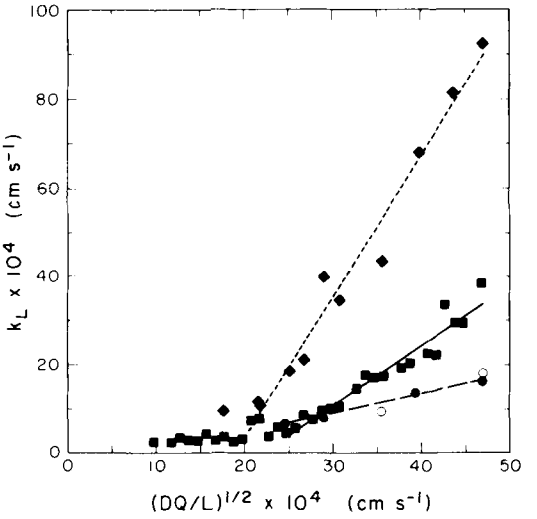


*Fig. 4.* Plot of $k_L$ data for the model of Fortescue and Pearson (1967), $k_L$ versus $(DQ/L)^{1/2}$. ◆, represent average value of 4 independent determinations of $k_L$ for a rayon/vacuum cleaned interface. Small dashed line is linear regression for $(DQ/L)^{1/2} \times 10^4 > 20$ cm s$^{-1}$ with $m = 3.2$, $r = 0.99$. ■, represent average value of at least 4 independent measurements of $k_L$ for a lens paper cleaned interface. Solid line is linear regression for $(DQ/L)^{1/2} \times 10^4 > 25$ cm s$^{-1}$ with $m = 1.4$, $r = 0.96$. ●, represent averages of 4 independent determinations of $k_L$ for an interface covered by a 1-octadecanol monolayer. Large dashed line is linear regression with $m = 0.45$, $r = 0.99$. ○, represent average of 4 independent determinations of $k_L$ for an uncleaned interface.

If this hypothesis is correct the transition observed in the stirred-tank data is analogous to that found in plots of $k_L$ versus wind speed or friction velocity from wind tunnel data (Broecker et al., 1978; Liss et al., 1981). There the transition is thought to be due to the onset of capillary waves and concomitant change from a smooth to rough aerodynamic surface. This alters the functional dependence of $k_L$ on aerodynamic parameters in a manner analogous to differences observed between the clean interface case embodied by (6) and the film-covered theory

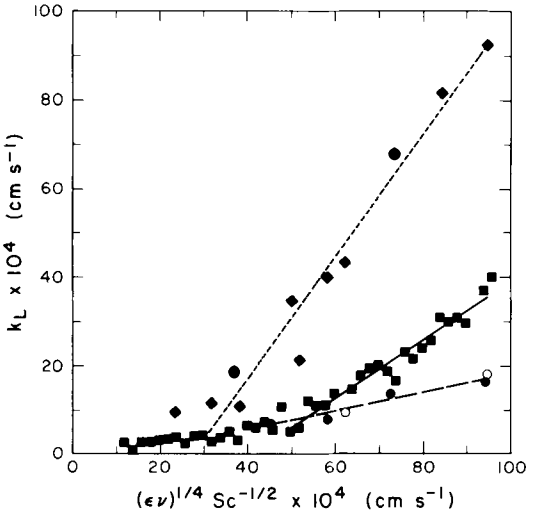


*Fig. 5.* Plot of $k_L$ for Lamont and Scott (1970) model, $k_L$ versus $(\varepsilon\nu)^{1/4}Sc^{-1/2}$. ◆, $k_L$ data for rayon/vacuum cleaned interface plotted as in Fig. 4. Small dashed line is linear regression for $(\varepsilon\nu)^{1/4}Sc^{-1/2} \times 10^4 > 30$ cm $s^{-1}$ with $m = 1.4$ and $r = 0.98$. ■, $k_L$ data for lens paper cleaned interface plotted as in Fig. 4. Solid line is linear regression for $(\varepsilon\nu)^{1/4}Sc^{-1/2} \times 10^4 > 50$ cm $s^{-1}$ with $m = 0.65$, $r = 0.97$. ●, $k_L$ data for 1-OD film covered interface plotted as in Fig. 4. Large dashed line, linear regression with $m = 0.21$, $r = 0.97$. ○, $k_L$ data for uncleaned interface plotted as in Fig. 4.

formulated by (9). In other words, the transition in the present stirred-tank data might be due to a fundamental change in the fluid mechanical dependence of the transport process.

The major difference between the two cleaned surface data sets is the slope of the high turbulence intensity data. The slope of the rayon/vacuumed-cleaned results is much greater than that of the lens paper-cleaned data. Since surface films tend to decrease $k_L$ for a given turbulence intensity (Davies, 1972), the difference in slopes suggests that the rayon/vacuum technique produced a cleaner aqueous surface. However, due to the presence of the transition in slope in the data set it cannot be concluded that the rayon/vacuum-cleaned surfaces were entirely free of spontaneously generated interfacial films.

The 1-OD film data have a much lower slope than either of the cleaned-surface data sets and no transition was observed. This lack of transition suggests that the hydrodynamical dependence of $k_L$ was constant over the range of turbulence intensities studied. Also, all the data sets appear to be equivalent for low turbulence intensities. This supports the hypothesis that the cleaned interfaces were contaminated by weak surface films. However, since the slopes of the cleaned and film-covered interface data sets are different for the high turbulence regime, it is assumed that the cleaned surfaces were hydrodynamically different from the film-covered surfaces.

Experiments done with no surface cleaning at all resulted in measured $k_L$ values which were very similar to the 1-OD results. This showed the significance of removal of the adventitious surface films prior to the measurement of $k_L$. It also demonstrates the sensitivity of a liquid-phase rate controlled gas/liquid transport process to the presence of interfacial films.

Use of the film-covered gas/liquid transport model embodied by (9) resulted in poor prediction of the $k_L$ values for the 1-OD film data. This result shows that even a severely film-contaminated gas/liquid interface does not behave exactly like a solid/liquid interface with respect to mass transfer.

In conclusion, both the large eddy and the dissipation model correlate with the data equally well in the high turbulence regime and no preferential choice can be made between them. The transitions in $k_L$ observed in the cleaned-surface experiments might have been due to a change in the fluid mechanical dependence of $k_L$. This change was presumably caused by the presence of weak surface films. Alternatively, the transition in the $k_L$ data may have been caused by (10) and (12) inadequately describing the behavior of weak turbulence in the presence of a gas/liquid interface. Unfortunately, this problem cannot be resolved at the present time. It is the subject of further research in this laboratory.

Even though one model cannot be preferred over the other on the basis of the present data, the dissipation model is advantageous in that it allows our results to be compared to other types of gas-transfer experiments.

## 6. Comparison to wind tunnel data

As stated above, the ultimate goal of this type of research is the prediction of gas-transport

coefficients in oceans, lakes etc. Tanks stirred by oscillating grids trade simulation of environmental wind/wave conditions for known, characterized turbulence. Since wind tunnels simulate these conditions more closely, it seems desirable to compare $k_L$ measurements made in them to the present stirred-tank results. The dissipation model of Cohen (1983) may be used to relate our data to the wind tunnel experiments of Broecker et al. (1978), Liss et al. (1981), Mackay and Yeun (1983), Merlivat and Memery (1983), and Jähne et al. (1984).

Cohen (1983) divides $\varepsilon$ into a mechanically generated component $\varepsilon_s$, a wave generated component $\varepsilon_w$, and a component due to the wind induced drift current $\varepsilon_d$ with

$$\varepsilon_w = 0.4\nu A'^4 \kappa^4 \sigma^2, \quad (17)$$

$$\varepsilon_d = 3.25 \times 10^{-4} (U_w^*)^4/\nu, \quad (18)$$

where $A'$ (cm) is the wave amplitude, $\kappa$ (cm$^{-1}$) and $\sigma$ (s$^{-1}$) are the radian wave number and frequency respectively, and $U_w^*$ (cm s$^{-1}$) is the water side friction velocity. By assuming continuity of stress at the interface $U_w^*$ may be written as

$$U_w^* = (\rho_a/\rho_w)^{1/2} U_a^* \quad (19)$$

where $\rho_a$ (g cm$^{-3}$) and $\rho_w$ (g cm$^{-3}$) are the densities of air and water respectively, and $U_a^*$ (cm s$^{-1}$) is the air side friction velocity. This model assumes that there are no breaking waves. Cohen (1983) showed that if there is no mechanically-generated turbulence and $U_w^* > 2$ cm s$^{-1}$, then $\varepsilon_d \gg \varepsilon_w$ and $\varepsilon$ is determined mainly by $\varepsilon_d$. Assuming that $\varepsilon = \varepsilon_d$ for $U_w^* < 2$ cm s$^{-1}$ does not drastically underestimate $\varepsilon^{1/4}$. Cohen (1983) showed that for $U_w^* = 0.5$ cm s$^{-1}$, $\varepsilon_w = 0.45\varepsilon_d$. Neglecting this term in calculating $\varepsilon$ led to an 18% underestimation of the square root of the renewal rate $s$, i.e. $(\varepsilon/\nu)^{1/4}$ which is acceptable for the present comparisons. In support of this assumption, substitution of (20) into (6) shows that $k_L$ should correlate linearly with $U_w^*$. This result has been derived separately by Münnich and Flothman (1975) and Deacon (1977) and also observed experimentally (Cohen, 1983).

This model was used to compare the present data for $CO_2$ in a grid-stirred tank to the wind tunnel data of Broecker et al. (1978) for $CO_2$, Liss et al. (1981) for $O_2$, Mackay and Yeun (1983) for benzene, toluene and 1,2-dichloropropane, Merlivat and Memery (1983) for $N_2O$, and Jähne et al. (1984) for $CO_2$. For the wind tunnel data, $\varepsilon$ was calculated from reported values of $U_a^*$ or $U_w^*$ and (18) and (19). The $k_L$ data for the different experiments were normalized to Sc = 600 as in Jähne et al. (1984) to correct for differences in diffusivities and temperatures. These values were then plotted versus $(\varepsilon/\nu)^{1/4}$ and the results are shown in Fig. 6.

The data sets for clean gas/liquid interfaces of Broecker et al. (1978), Liss et al. (1981), Merlivat and Memery (1983) and Jähne et al. (1984) all correlate reasonably well with the rayon/vacuum-cleaned grid results. While there is considerable scatter among the data sets, Fig. 6 is very encouraging. It suggests that Cohen's model may be used to relate stirred tank results to wind tunnel experiments provided the aqueous surface is free

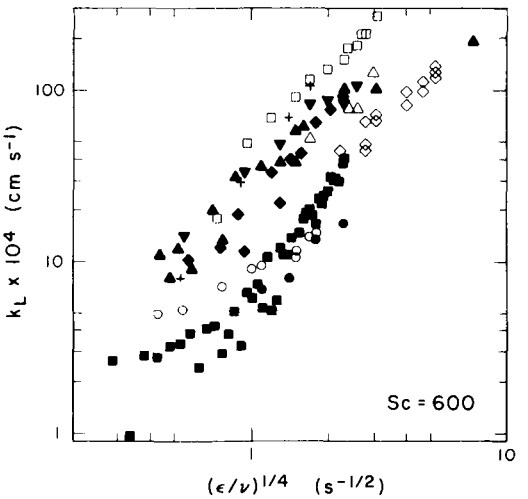


*Fig. 6.* Plot of normalized data $k_L$ data versus $(\varepsilon/\nu)^{1/4}$ for the present grid data and wind tunnel results. $\varepsilon$ for the wind tunnel data was calculated from the model of Cohen (1983) using (18) and (19). The data shown are: ◆, $CO_2$, rayon/vacuum cleaned interface, present grid data; ■, $CO_2$, lens paper cleaned interface, present grid data; ●, $CO_2$, 1-octadecanol film, present grid data; ○, $CO_2$, circular wind tunnel, film covered interface, Jähne et al. (1984); □, $CO_2$, linear wind tunnel, clean interface, Broecker et al. (1978); +, $O_2$, linear wind tunnel, clean interface, Liss et al. (1981); ◇, Benzene, toluene, 1,2-dichloropropane, linear wind tunnel, clean interface, Mackay and Yeun (1983); ▼, $N_2O$, linear wind tunnel, clean interface, Merlivat and Memery (1983); ▲, $CO_2$, circular wind tunnels, clean interface, Jähne et al. (1984); △, $CO_2$, linear wind tunnel, clean interface, Jähne et al. (1984).

of surface films. Fig. 6 also provides evidence that wind-driven gas/liquid transport has the same hydrodynamical dependence as gas exchange governed by mechanically-generated turbulence.

The data of Mackay and Yeun (1983) and the lens paper-cleaned grid results are systematically lower than the other data sets but are in very good agreement with each other. As noted in the previous section, there is evidence that the $CO_2$/water interfaces in the lens paper-cleaned experiments were contaminated by surface films. The data set of Mackay and Yeun (1983) is unique in that it is the only data set included in this comparison which studied the transfer of organic material from an aqueous to a gaseous phase. The organic material added to the aqueous phase might have had surface active contaminants present which affected the transport rates through the formation of a surface film. If this were the case, it would explain the observed agreement of the Mackay and Yeun (1983) data with the lens paper cleaned set.

The 1-OD film results from the grid-stirred tank are in rough agreement with the film-covered wind tunnel results of Jähne et al. (1984). Also, the slopes of the two film-covered interface data sets are approximately the same. This suggests that the hydrodynamical dependence is the same in both cases.

In general, the model of Cohen (1983) shows hope of being able to relate wind tunnel experiments to studies done with mechancially generated turbulence. This is one step further in the understanding of the mechanism of wind-driven gas/liquid exchange. This preliminary result shows that the gas-exchange process in the two types of experiments may possibly be described by the same surface renewal model over a limited range of conditions (i.e., high turbulence intensity, no breaking waves). The model of Kitaigorodskii (1984) or Kerman (1984) for gas-exchange in the presence of breaking wind waves might be useful to further extend these results to even more realistic environmental conditions.

## 7. Conclusions

Our results show that for intense turbulence ($Re_t > 70$), either the large eddy or dissipation surface renewal model of gas/liquid transport correlates with measured values of $k_L$. This correlation breaks down for low turbulence intensities due to either inapplicability of the Hofinger and Toly (1975) results or a transition from renewal of the surface to a stagnant interface. Experiments done with no surface cleaning, an intentionally-created monolayer, and two types of surface cleaning procedures have shown that $k_L$ is very sensitive to the presence of interfacial films. The presence of interfacial films not only affects the absolute magnitude of $k_L$, but the functional dependence of $k_L$ on the turbulence parameters as well.

Preliminary results indicate that the model of Cohen (1983) might be useful in relating stirred-cell experiments with clean gas/liquid interfaces to wind tunnel $k_L$ data for moderate wind speeds with no breaking waves. It is hoped that further work in wind tunnels and stirred-cells will enable verification of this relation. If proven applicable, this model should be useful in estimating environmental values of $k_L$ for given wind/wave conditions.

While wind tunnel gas-exchange experiments will certainly continue to be useful, there are environmentally-important gas/liquid transport conditions which are more easily studied by use of grids. Grids may be better suited for the study of the effect of turbulence generated by buoyancy overturns on air/sea exchange. Another area of research is the continued study of the effect of surface films on gas/liquid transport. Since films are mobile at gas/liquid interfaces they are blown to the downwind end of linear wind tunnels (Broecker et al., 1978). Therefore, the effect of surface films on gas transfer may be more accurately studied in a windless tank where they remain stationary. Studies such as this together with continued work in wind-tunnels should provide a more complete picture of the complex environmental gas-exchange process.

## 8. Acknowledgements

The authors express their appreciation to T. D. Dickey and R. E. Breidenthal Jr. for many helpful discussions. Financial support for this work was provided in part by grants from the

National Oceanic and Atmospheric Administration (NOAA NA80RA00043) and the Donors of the Petroleum Research Fund, administered by the American Chemical Society (ACS/PRF 17154-AC7). The technical assistance of Lorne M. Isabelle and Frederick Thone is also gratefully acknowledged.

## REFERENCES

Ackgerman, A. and Gainer, J. L. 1972. Predicting gas-liquid diffusivities. *J. Chem. Eng. Data 17*, 372–377.

Balls, P. W. and Liss, P. S. 1983. Exchange of $H_2S$ between water and air. *Atmos. Environ. 17*, 735–742.

Bevington, P. R. 1969. *Data reduction and error analysis for the physical sciences*. N.Y./N.Y.: McGraw-Hill.

Broecker, H. C., Petermann, J. and Siems, W. 1978. The influence of wind on $CO_2$-exchange in a wind-wave tunnel, including the effects of monolayers. *J. Mar. Res. 36*, 595–610.

Brumley, B. 1984. Turbulence measurements near the free surface in stirred grid experiments. In *Gas-transfer at water surfaces* (eds. W. Brutsaert and G. H. Jirka). Hingham/MA: D. Reidel, 83–92.

Cohen, Y. 1983. Mass transfer across a sheared, wavy air-water interface. *Int. J. Heat Mass Trans. 26*, 1289–1297.

Crits, G. J. 1961. A simple test for trace organic substances in water. Symposium on analytical methods with emphasis on minor elements. *Am. Chem. Soc.*, September.

Danckwerts, P. V. 1970. *Gas-liquid reactions*. N.Y./N.Y.: McGraw-Hill.

Davies, J. T. 1972. *Turbulence phenomena*. N.Y./N.Y.: Academic Press.

Davies, J. T. and Lozano, F. J. 1979. Turbulence characteristics and mass transfer at air-water surfaces. *A.I.Ch.E.J. 25*, 405–415.

Deacon, E. L. 1977. Gas transfer to and across an air-water interface. *Tellus 29*, 363–374.

Dickey, T. D., Hartman, B., Hammond, D. and Hurst, E. 1984. A laboratory technique for investigating the relationship between gas transfer and fluid turbulence. In *Gas-transfer at water surfaces* (eds. W. Brutsaert and G. H. Jirka). Hingham/MA: D. Reidel, 93–101.

Fortescue, G. F. and Pearson, J. R. A. 1967. On gas absorption into a turbulent liquid. *Chem. Eng. Sci. 22*, 1163–1176.

Gibbons, B. H. and Edsall, J. T. 1963. Rate of hydration of carbon dioxide and dehydration of carbonic acid at 25°. *J. Biol. Chem. 238*, 3502–3507.

Higbie, R. 1935. The rate of absorption of a pure gas into a still liquid during short periods of exposure. *Trans. A.I.C.E. 35*, 365–389.

Hinze, J. O. 1975. *Turbulence, 2nd ed.* N.Y./N.Y.: McGraw-Hill.

Hopfinger, E. J. and Toly, J. A. 1976. Spatially decaying turbulence and its relation to mixing across density interfaces. *J. Fluid Mech. 78*, 155–175.

Hunt, J. C. R. and Graham, J. M. R. 1978. Free-stream turbulence near plane boundaries. *J. Fluid Mech. 84*, 209–235.

Jähne, B., Münnich, K. O. and Siegenthaler, U. 1979. Measurement of gas exchange and momentum transfer in a circular wind-water tunnel. *Tellus 31*, 321–329.

Jähne, B., Huber, W., Dutzi, A., Wais, T. and Ilmberger, J. 1984. Wind/wave-tunnel experiment on the Schmidt number and wave field dependence of air/water gas exchange. In *Gas-transfer at water surfaces* (eds. W. Brutsaert and G. H. Jirka). Hingham/MA: D. Reidel Publishers, 303–309.

Kerman, B. R. 1984. A model of interfacial gas transfer for a well-roughened sea. *J. Geophys. Res. 89D*, 1439–1446.

Kitaigorodskii, S. A. 1984. On the fluid dynamical theory of turbulent gas transfer across an air-sea interface in the presence of breaking wind-waves. *J. Phys. Oceanogr. 14*, 960–972.

Lamont, J. C. and Scott, D. S. 1970. An eddy cell model of mass transfer into the surface of a turbulent liquid. *A.I.Ch.E.J. 16*, 513–519.

Lindqvist, L. 1960. A flash photolysis study of fluorescein. *Arkiv. Kemi. 16*, 79–138.

Liss, P. S. 1983. Gas transfer: experiments and geochemical implications. In *Air-sea exchange of gases and particles* (eds. P. S. Liss and W. G. N. Slinn). Hingham/MA: D. Reidel publishers, 241–298.

Liss, P. S., Balls, P. W., Martinelli, F. N. and Coantic, M. 1981. The effect of evaporation and condensation on gas transfer across an air-water interface. *Oceanologica Acta 4*, 129–138.

Lytle, F. E. 1982. Laser excited molecular fluorescence of solutions. *J. Chem. Ed. 59*, 915–920.

Mackay, D. and Yeun, A. T. K. 1983. Mass transfer coefficient correlations for volatilization of organic solutes from water. *Env. Sci. Tech. 17*, 211–217.

Mellor, G. L. 1973. Analytic prediction of the properties of stratified planetary surface layers. *J. Atmos. Sci. 30*, 1061–1069.

Merlivat, L. and Memery, L. 1983. Gas exchange across an air-water interface: experimental results and modeling of bubble contribution to transfer. *J. Geophys. Res. 88C*, 707–724.

Münnich, K. O. and Flotham, D. 1975. Gas exchange in relation to other air/sea interaction phenomena. SCOR workshop on "Air/sea interaction phenomena" Miami, Dec. 8–12, 1975. (Background papers prepared for the Ocean Sciences Board, Natl. Res. Council, Wash. D.C., 1977.)

Ohkuma, S. and Poole, B. 1978. Fluorescence probe measurement of intralysomal pH in living cells and perturbation of the pH by various agents. *Proc. Natl. Acad. Sci. USA 75*, 3327–3331.

Pankow, J. F., Asher, W. E. and List, E. J. 1984. Carbon dioxide transfer at the gas/water interface as a function of system turbulence. In *Gas-transfer at water surfaces* (eds. W. Brutsaert and G. H. Jirka). Hingham/MA: D. Reidel Publishers, 101–113.

Stumm, W. and Morgan, J. J. 1982. *Aquatic chemistry, 2nd edition*. N.Y./N.Y.: J. Wiley.

Tennekes, H. and Lumley, J. L. 1972. *A first course in turbulence*. Cambridge/MA: MIT Press.

Thompson, S. M. and Turner, J. S. 1975. Mixing across an interface due to turbulence generated by an oscillating grid. *J. Fluid Mech. 67*, 349–369.

Whitman, W. G. 1923. Preliminary experimental confirmation of the two-film theory of gas adsorption. *Chem. Metall. Eng. 29*, 146–148.